Modeling Pc4 Pulsations in Two and a Half Dimensions

DRAFT VERSION CREATED ON FEBRUARY 7, 2016

Acknowledgements

Acknowledgement placeholder.

Dedication

Dedication placeholder.

Abstract

Abstract placeholder.

Contents

List of Tables

List of Figures

Chapter 1

The Near-Earth Environment

It's all about energy transfer!

Some example citations, including a few with special characters: [1], [2], [3].

Sun generates energy through nuclear reactions.

This energy drives behavior in the near-Earth environment.

Typical solar wind density is $\sim 5\,/\mathrm{cm}^3$. Typical solar wind velocity at Earth is $10^2\,\mathrm{km/s}$ to $10^3\,\mathrm{km/s}$. Typical solar wind particle energy is 1 keV to 10 keV. Density can vary by ∼3 orders of magnitude, and velocity by one, during times of high solar activity. CMEs can also mess with the north/south component of the interplanetary magnetic field.

45° angle with the Earth-Sun line, which is the X direction. [1]

Solar wind is what deforms Earth's magnetic field to form the magnetosphere.

Transient solar wind phenomena, such as coronal mass ejections, are also known to be related to geomagnetic disturbances at Earth. Jesse cites here:

R. L. McPherron. Physical processes producing magnetospheric substorms and mangetic

[1] We use uppercase X, Y, and Z to indicate GSE coordinates: X points from the Earth to the Sun. Y is perpendicular to X, and in the Sun's ecliptic plane, pointing duskwards... against Earth's orbital motion. Points north, out of the ecliptic plane. Later, we will use lowercase x, y, and z to define a more-or-less analogous corodinate system with respect to Earth.

storms. In J. A. Jacobs, editor, Geomagnetism, volume 4, chapter 7. Academic Press, 1991.

G. Rostoker. Substorms. In Handbook of the Solar-Terrestrial Environment, chapter 15. Springer-Verlag, 2007.

This might just be worth tracking down... Jesse cites several chapters:

M. Shulz. Magnetospheres. In Handbook of the Solar-Terrestrial Environment, chapter 7. Springer-Verlag, 2007.

1.1 The Outer Magnetosphere

The outer magnetosphere is a region where the field lines are closed, but significantly deformed by the solar wind.

1.1.1 The Magnetopause

1.1.2 The Magnetotail

1.1.3 Cusp Regions

1.2 The Inner Magnetosphere

In the inner magnetosphere, field lines are closed, and are approximately dipolar.

1.2.1 The Plasmasphere

1.2.2 Ring Currents

1.2.3 The Radiation Belts

1.3 Geomagnetic Disturbances

1.3.1 Storms

1.3.2 Substorms

Chapter 2

Pc4 Pulsations

TODO: Fujita and Tamao 1988, Greifinger and Greifinger 1968, 1973 showed that the poloidal and toroidal modes act differently at the ionosphere.

TODO: Hughes 1974: Hall conducting ionosphere reflects ULF wave fields. Well-known result.

TODO: Theoretical consideration of decay vs propagation, by frequency. Lysak and Yoshikawa 2006.

TODO: Takahashi 2013 saw a high-modenumber poloidal mode with THEMIS.

TODO: Fishbone instability. McGuire 1983, Chen 1984. Similar phenomenon, but for lab plasmas.

2.1 Observations

Dai noted specifically that it was unclear why poloidal Pc4 pulsations were preferrentially seen on the dayside, since drift resonance should be azimuthally distributed.

2.2 Theoretical Work

2.3 Giant Pulsations

Chapter 3

Waves in Cold Resistive Plasmas

Cold, linearlized Ampère's Law and Faraday's Law. The vector $\underline{B}$ is the perturbation to the zeroth-order magnetic field.

$$\frac{\partial}{\partial t}\underline{B} = -\nabla\times\underline{E} \qquad \underline{\underline{\epsilon}}\cdot\frac{\partial}{\partial t}\underline{E} = \frac{1}{\mu_0}\nabla\times\underline{B} - \underline{J} \tag{3.1}$$

Ohm's Law. Electron inertial effects are included in the parallel direction. See chapter 5.

$$\frac{m_e}{ne^2}\frac{\partial}{\partial t}J_{\|} = \sigma_0 E_{\|} - J_{\|} \qquad 0 = \underline{\underline{\sigma}}_{\perp}\cdot\underline{E}_{\perp} - \underline{J}_{\perp} \tag{3.2}$$

Suppose that the fields and currents are resonating as $\exp(i\underline{k}\cdot\underline{x} - i\omega t)$. Evaluate the derivatives. Eliminate magnetic fields and currents.

$$0 = E_{\|} + \frac{c^2}{\omega^2}\left(\underline{k}\,\underline{k}\cdot\underline{E} - k^2\underline{E}\right)_{\|} + \frac{i\omega_P^2}{\omega\left(\nu - i\omega\right)}E_{\|} \tag{3.3}$$

$$0 = \underline{E}_{\perp} + \frac{v_A^2}{\omega^2}\left(\underline{k}\,\underline{k}\cdot\underline{E} - k^2\underline{E}\right)_{\perp} + \frac{i}{\epsilon_{\perp}\omega}\underline{\underline{\sigma}}_{\perp}\cdot\quad\underline{E}_{\perp} \tag{3.4}$$

The above expression makes use of the vector identity $\underline{k}\times\underline{k}\times\underline{E} = \underline{k}\,\underline{k}\cdot\underline{E} - k^2\underline{E}$. The Alfvén speed, speed of light, plasma frequency, and parallel conductivity are defined in the usual way:

$$v_A^2 \equiv \frac{1}{\mu_0 \epsilon_\perp} \qquad c^2 \equiv \frac{1}{\mu_0 \epsilon_0} \qquad \omega_P^2 \equiv \frac{ne^2}{m_e \epsilon_0} \qquad \sigma_0 \equiv \frac{ne^2}{m_e \nu} \tag{3.5}$$

Note that this definition of the Alfvén speed takes into account the displacement current correction which is important when v_A approaches c.

Without loss of generality, the wave vector $\underline{k}$ can be said to lie in the x-z plane; the distinction between the x and y directions is revisited in section 3.4. Let θ be the angle between $\underline{k}$ and the zeroth-order magnetic field.

Then equations (3.3) and (3.4) can be combined into the usual dispersion tensor form, $\underline{\underline{T}} \cdot \underline{E} = 0$, where

$$\underline{\underline{T}} = \underline{\underline{\mathbb{I}}} + \frac{k^2}{\omega^2} \begin{bmatrix} -v_A^2 \cos^2\theta & 0 & v_A^2 \sin\theta\cos\theta \\ 0 & -v_A^2 & 0 \\ c^2 \sin\theta\cos\theta & 0 & -c^2\sin^2\theta \end{bmatrix} + \frac{i}{\omega} \begin{bmatrix} \frac{\sigma_P}{\epsilon_\perp} & -\frac{\sigma_H}{\epsilon_\perp} & 0 \\ \frac{\sigma_H}{\epsilon_\perp} & \frac{\sigma_P}{\epsilon_\perp} & 0 \\ 0 & 0 & \frac{\omega_P^2}{\nu - i\omega} \end{bmatrix} \tag{3.6}$$

Nontrivial solutions exist only when $\left|\underline{\underline{T}}\right| = 0$. This gives rise to a seventh-order polynomial in ω, so it's necessary to consider limits of particular interest.

3.1 Parallel Propagation Limit

Parallel propagation is a naive representation of a field line resonance; the wave vector moves energy along the field line. Taking $\theta = 0$, $\underline{\underline{T}}$ simplifies to

$$\underline{\underline{T}}_\parallel = \underline{\underline{\mathbb{I}}} - \frac{k^2 v_A^2}{\omega^2} \begin{bmatrix} 1 & 0 & 0 \\ 0 & 1 & 0 \\ 0 & 0 & 0 \end{bmatrix} + \frac{i}{\omega} \begin{bmatrix} \frac{\sigma_P}{\epsilon_\perp} & -\frac{\sigma_H}{\epsilon_\perp} & 0 \\ \frac{\sigma_H}{\epsilon_\perp} & \frac{\sigma_P}{\epsilon_\perp} & 0 \\ 0 & 0 & \frac{\omega_P^2}{\nu - i\omega} \end{bmatrix} \tag{3.7}$$

Conveniently, parallel and perpendicular polarizations are not coupled in equation (3.7).

3.1.1 Parallel Polarization

The parallel component of the determinant of equation (3.7) gives

$$\omega^2 + i\nu\omega - \omega_P^2 = 0 \tag{3.8}$$

With no k dependence this expression doesn't describe a wave per se, so much as a resonant frequency. Solving directly,

$$\omega = -\frac{i\nu}{2} \pm \sqrt{\omega_P^2 - \frac{\nu^2}{4}} \tag{3.9}$$

The plasma frequency significantly exceeds the collision frequency everywhere except a narrow strip at the ionospheric boundary of the model. Expanding in large ω_P gives

$$\omega^2 = \omega_P^2 - i\nu\omega_P + ... \tag{3.10}$$

TODO: Actually, double-check this. How does ν compare to ω_P at the ionospheric boundary when there is no Boris factor?

This is the plasma oscillation.

3.1.2 Perpendicular Polarization

The perpendicular components of the determinant of equation (3.7) give

$$\omega^4 + 2i\frac{\sigma_P}{\epsilon_\perp}\omega^3 - \left(2k^2v_A^2 + \frac{\sigma_P^2 + \sigma_H^2}{\epsilon_\perp^2}\right)\omega^2 - 2ik^2v_A^2\frac{\sigma_P}{\epsilon_\perp}\omega + k^4v_A^4 = 0 \tag{3.11}$$

This can be solved in exact form. Noting that $\pm$ and $\bigoplus$ are independent,

$$\omega = \left(\frac{\pm\sigma_H - i\sigma_P}{2\epsilon_\perp}\right) \bigoplus \sqrt{k^2v_A^2 + \left(\frac{\pm\sigma_H - i\sigma_P}{2\epsilon_\perp}\right)^2} \tag{3.12}$$

Over the vast majority of a field line, $kv_A \gg \frac{\sigma_P}{\epsilon_\perp}$ and $kv_A \gg \frac{\sigma_H}{\epsilon_\perp}$.

$$\omega^2 = k^2 v_A^2 \oplus kv_A \frac{\sigma_H \pm i\sigma_P}{\epsilon_\perp} + ... \tag{3.13}$$

This is the Alfvén wave, evidently split by the ionospheric conductivity, propagating along the zeroth-order magnetic field line.

3.2 Perpendicular Propagation Limit

A wave's ability to propagate across field lines is also of interest. When $\theta = \frac{\pi}{2}$, $\underline{\underline{T}}$ simplifies to

$$\underline{\underline{T}}_\perp = \underline{\underline{\mathbb{I}}} - \frac{k^2}{\omega^2}\begin{bmatrix} 0 & 0 & 0 \\ 0 & v_A^2 & 0 \\ 0 & 0 & c^2 \end{bmatrix} + \frac{i}{\omega}\begin{bmatrix} \frac{\sigma_P}{\epsilon_\perp} & -\frac{\sigma_H}{\epsilon_\perp} & 0 \\ \frac{\sigma_H}{\epsilon_\perp} & \frac{\sigma_P}{\epsilon_\perp} & 0 \\ 0 & 0 & \frac{\omega_P^2}{\nu - i\omega} \end{bmatrix} \tag{3.14}$$

As in the parallel propagation case, the parallel and perpendicular components of the determinant are decoupled.

3.2.1 Parallel Polarization

The parallel component of the determinant of equation (3.14) gives

$$\omega^3 + i\nu\omega^2 - \left(k^2c^2 + \omega_P^2\right)\omega - ik^2c^2\nu = 0 \tag{3.15}$$

The above expression can be solved exactly, but the resulting expressions are too long to be useful.

Expanding the solution in large ω_P gives the O mode: a compressional wave with a parallel electric field.

$$\omega^2 = k^2c^2 + \omega_P^2 - i\nu\omega_P + ... \tag{3.16}$$

3.2.2 Perpendicular Polarization

The perpendicular components of the determinant of equation (3.14) give

$$\omega^3 + 2i\frac{\sigma_P}{\epsilon_\perp}\omega^2 - \left(2k^2v_A^2 + \frac{\sigma_P^2 + \sigma_H^2}{\epsilon_\perp^2}\right)\omega - ik^2v_A^2\frac{\sigma_P}{\epsilon_\perp} = 0 \tag{3.17}$$

Again, the roots of the cubic are impractically long.

Expanding in large conductivity, as is expected near the ionospheric boundary, gives

$$\omega^2 = k^2v_A^2 + \left(\frac{\sigma_H \pm i\sigma_P}{\epsilon_\perp}\right)^2 + ... \tag{3.18}$$

Whereas expanding in small conductivity, as is expected far from the boundary, gives

$$\omega^2 = k^2v_A^2 \pm ikv_A\frac{\sigma_P}{\epsilon_\perp} + ... \tag{3.19}$$

Both of which are Alfvén waves.

3.3 High Altitude Limit

At high altitude, where the density is very low compared to the ionosphere, it's reasonable to approximate $\sigma_P \to 0$ and $\sigma_H \to 0$ and $\nu \to 0$.

In this case, $\underline{\underline{T}}$ simplifies to

$$\underline{\underline{T}}_\infty = \underline{\underline{\mathbb{I}}} - \frac{k^2}{\omega^2}\begin{bmatrix} v_A^2\cos^2\theta & 0 & -v_A^2\sin\theta\cos\theta \\ 0 & v_A^2 & 0 \\ -c^2\sin\theta\cos\theta & 0 & c^2\sin^2\theta \end{bmatrix} - \frac{\omega_P^2}{\omega^2}\begin{bmatrix} 0 & 0 & 0 \\ 0 & 0 & 0 \\ 0 & 0 & 1 \end{bmatrix} \tag{3.20}$$

In this case it's the azimuthal polarization that decouples from the other two.

3.3.1 Azimuthal Polarization

The azimuthal component of the determinant of equation (3.20) simply gives the Alfvén wave.

$$\omega^2 = k^2 v_A^2 \tag{3.21}$$

3.3.2 Meridional Polarization

The components of the determinant of equation (3.20) which fall in the meridional plane give, taking $k_\perp \equiv k \sin\theta$ and $k_\| \equiv k \cos\theta$,

$$\omega^4 - \left(k_\|^2 v_A^2 + k_\perp^2 c^2 + \omega_P^2\right)\omega^2 + k_\|^2 v_A^2 \omega_P^2 = 0 \tag{3.22}$$

The above expression is quadratic in ω^2, and thus can be solved directly.

$$\omega^2 = \frac{1}{2}\left(k_\|^2 v_A^2 + k_\perp^2 c^2 + \omega_P^2\right) \pm \sqrt{\frac{1}{4}\left(k_\|^2 v_A^2 + k_\perp^2 c^2 + \omega_P^2\right)^2 - k_\|^2 v_A^2 \omega_P^2} \tag{3.23}$$

Noting that ω_P is very large, the two roots simplify to

$$\omega^2 = k_\|^2 v_A^2 + \ldots \tag{3.24}$$

$$\omega^2 = k_\|^2 v_A^2 + k_\perp^2 c^2 + \omega_P^2 + \ldots \tag{3.25}$$

3.4 Implications for This Work

3.4.1 Mode Coupling

TODO: Have we got enough/appropriate math here to talk about how σ_H rotates fields at the ionosphere? Doubtful.

3.4.2 High Modenumber Cutoff

As m becomes large, it puts a lower bound on the modenumber, and thus on the frequency. For an Alfvén wave, $\omega^2 = k^2 v_A^2$,

$$k \geq k_\phi = \frac{m}{2\pi r} \qquad \text{so} \qquad \omega \geq \frac{m}{2\pi r} v_A \tag{3.26}$$

Any wave with a frequency below this threshold will become evanescent.

Chapter 4

Numerical Model

The model works in two and a half dimensions. A meridional slice of the magnetosphere is resolved. Fields are presumed to vary azimuthally according to a fixed modenumber m . Derivatives in ϕ are replaced by im. Imaginary field values indicate a phase shift in the azimuthal direction.

TODO: Note that Lysak's 2013 paper[4] was 2.5D.

The use of a fixed modenumber allows a dramatic decrease in computational cost. Waves with very high azimuthal modenumber are prohibitively expensive to simulate since they can only be resolved if grid resolution is very fine in the azimuthal direction.

TODO: Has anyone actually talked about computational expense as a constraint on high-m simulations?

This prevents the simultaneous consideration of dayside and nightside phenomena, but is fine for azimuthally-localized waves. As was shown by [5], and recently confirmed in detail by [2], Pc4 pulsations are generally confined to just a few hours MLT on the dayside.

Driving with a compressional pulse from the outer boundary of a simulation is typical. This model also includes a novel driving mechanism: perturbations to the ring current.

The code is linear. All magnetic fields are a first-order perturbation over the zeroth-order dipole field. This is a not-great assumption out towards the magnetopause. In practice, however, most activity is within $L \sim 7\,\mathrm{R_E}$, where the dipole approximation is pretty good.

Models with height-resolved ionospheres are a very recent development. Lysak presented his in 2013[4].

Ground signatures are fairly recent as well.

TODO: Some ground signature work as far back as Greifinger and Greifinger in 1968, but there's been steady advancement. Lysak and Song, in 2006, were the first to work out ground signatures without the assumption of a single-frequency wave.

TODO: The support software – the driver and the plotter – are significant too. Do they go in a section? In an appendix?

TODO: Past FLR simulations focused on a single mode, didn't account well for the ionosphere, etc. Lee and Lysak 1989, 1990, 1991, Rankin et al 1993, 1995, 1999, Tikhonchuk and Rankin 2000, 2002.

TODO: Past work that got ground signatures (without latitude-dependent zenith angle) Greifinger and Greifinger 1968, 1973, Hughes 1974, Sciffer and Waters 2002, Sciffer et al 2005. Better computation of ground signatures... Waters and Sciffer 2008, Sciffer and Waters 2011, Woodroffe and Lysak 2012.

Note that the model uses Mm, s, MC, and g as the fundamental units of length, time, charge, and mass respectively. As a result, electric field is measured in mV/m, magnetic field is measured in nT, and Poynting flux is measured in mW/m^2.

4.1 Coordinate System

When referring to fields in place, it's convenient to use lowercase[1] x, y, and z in their usual dipolar sense. The unit vector $\hat{z}$ is aligned with the dipole field (pointing outward in the northern hemisphere and inward in the southern hemisphere), while $\hat{x}$ is

[1] Not to be confused with uppercase X, Y, and Z, which orient relative to the sun; see chapter 1

perpendicular to $\hat{z}$ within the meridional plane and $\hat{y}$ points in the azimuthal direction.

TODO: Double-check the signs for x (radially inward or outward at the equator?) and y (east or west?).

TODO: Wait... are x, y, and z the same as Radoski's coordinates?

It's convenient to align the grid with the zeroth-order magnetic field, which is presumed to be a perfect dipole. Field line resonances (such as Pc4 pulsations) are guided by magnetic field lines.

TODO: Who showed that ULF waves can be guided? Cite them.

A typical outermost field line has an equatorial radius of $10\,\mathrm{R_E}$. At this point, the ideal dipole approximation is suspect, particularly on the dayside. In practice, however, most wave activity is concentrated around $L \sim 7$.

TODO: Discuss, in Future Work, how the grid would be generalized.

Radoski did theoretical work in the following dipole coordinates[6].

$$\mu = -\frac{\sin^2\theta}{r} \qquad\qquad \phi = \phi \qquad\qquad \nu = \frac{\cos\theta}{r^2} \tag{4.1}$$

TODO: The symbol ν is overused. Reserve it for collision frequency. Use something else here.

It's also convenient to take into account the effects of the ionosphere, the lower boundary of which is governed by gravity, and thus has a more-or-less constant altitude. If the above coordinates are used, no line of constant ν coincides with the ionosphere, at least not over a significant range of latitudes.

Many previous works have used an effective ionosphere of nonuniform altitude.

TODO: Figure out which previous works are worth citing here. Options include Radoski 1967, Lee and Lysak 1989, 1991, Rankin et al 1993, 1994, Streltsov and Lotko 1995, 1999.

TODO: "The ionosphere is important for Alfvén waves." Cite this.

In order to accommodate dipole field lines as well as a fixed-altitude ionosphere, a nonorthogonal grid is necessary. Such a grid was worked out numerically by Proehl[7], then formalized analytically by Lysak[8]:

$$u^1 = -\frac{R_I}{r}\sin^2\theta \qquad\qquad u^2 = \phi \qquad\qquad u^3 = \frac{R_I^2}{r^2}\frac{\cos\theta}{\cos\theta_0} \tag{4.2}$$

The term R_I indicates the ionosphere's position relative to Earth's center. It's generally taken to be $1\,\mathrm{R_E} + 100\,\mathrm{km}$.

Like μ and ϕ , the coordinates u^1 and u^2 index a field line. However, compared to ν , u^3 has been renormalized by $\cos\theta_0$, where θ_0 is the colatitude where each field line intersects the ionosphere in the northern hemisphere. As a result, for all field lines, $u^3 = \pm 1$ at the northern and southern foot points.

In terms of the McIlwain parameter, $u^1 = -\frac{R_I}{L}$, and $\cos\theta_0 = \sqrt{1 - \frac{R_I}{L}}$

Compared to equation (4.1), equation (4.2) represents a renormalization of indexing along each field line. The field lines themselves are not deformed.

TODO: Explain how we set up the grid. It should only take a paragraph or two – it doesn't need its own section.

TODO: Plot of the grid setup!

4.1.1 Covariant and Contravariant Bases

The coordinates defined in equation (4.2) are not orthonormal. As a result, it's necessary to consider covariant and contravariant basis vectors separately.

Covariant basis vectors $e_i \equiv \frac{\partial}{\partial u^i}\underline{x}$ are normal to the curve defined by constant u^i.

Contravariant basis vectors $e^i \equiv \frac{\partial}{\partial \underline{x}}u^i$ are tangent to the coordinate curve. Equally, they're normal to the plane defined by constant u^j for all $j \neq i$.

The basis vectors are reciprocal to one another[9], and can be used to define the metric tensor g.

$$\hat{e}^i \cdot \hat{e}_j = \delta^i_j \qquad \hat{e}_i \cdot \hat{e}_j = g_{ij} \qquad \hat{e}^i \cdot \hat{e}^j = g^{ij} \tag{4.3}$$

Note δ^i_j is the Kronecker delta, ε^{ijk} is the Levi-Civita symbol, and summation is implied over repeated indeces per Einstein's convention[10].

The metric tensor is used to map between the covariant and contravariant representations of a vector

$$A_i = g_{ij} A^j \qquad A^i = g^{ij} A_j \qquad \text{where} \qquad A_i \equiv \underline{A} \cdot \hat{e}_i \qquad A^i \equiv \underline{A} \cdot \hat{e}^i \tag{4.4}$$

The Jacobian, used for mapping differential volume elements between bases, can be expressed as the square root of the determinant of the metric tensor.

$$G = \sqrt{\varepsilon^{ijk} g_{1i} g_{2j} g_{3k}} \qquad \text{where} \qquad G du^1 du^2 du^3 = dV \tag{4.5}$$

This quantity is also used when expressing a curl or cross product in generalized coordinates.

$$(\nabla \times \underline{A})^i = \frac{\varepsilon^{ijk}}{G} \frac{\partial}{\partial u^j} A_k \qquad (\underline{A} \times \underline{B})^i = \frac{\varepsilon^{ijk}}{G} A_j B_k \tag{4.6}$$

4.1.2 Mapping to Physical Coordinates

The full expression for the basis vectors, metric tensor, and Jacobian determinant discussed in section 4.1.1 can be found in the appendix of [8].

TODO: These expressions should probably be written out an in appendix here too...

The basis vectors can be renormalized to produce unit vectors along the dipole coordinates x, y, and z.

$$\hat{x} = \frac{1}{\sqrt{g^{11}}} \hat{e}^1 \qquad \hat{y} = \frac{1}{\sqrt{g^{22}}} \hat{e}^2 \qquad \hat{z} = \frac{1}{\sqrt{g_{33}}} \hat{e}_3 \tag{4.7}$$

In addition, this coordinate system provides horizontal and radial unit vectors. Note that equation (4.8) is valid only at the ionospheric boundary.

$$\hat{\theta} = \frac{1}{\sqrt{g_{11}}}\hat{e}_1 \qquad \hat{\phi} = \frac{1}{\sqrt{g_{22}}}\hat{e}_2 \qquad \hat{r} = \frac{1}{\sqrt{g^{33}}}\hat{e}^3 \tag{4.8}$$

4.2 Ionospheric Profile

The ionospheric profiles used in this model are based on values tabulated in the Appendix B of Kelley's book[11]. They were adapted by Lysak[4] to take into account the effect of the magnetosphere's latitude-dependent density profile.

Mean molecular mass of 28 u at 100 km, 16 u around 400 km, down to 1 u above 1400 km.

Simulations are carried out using four profiles: active day, quiet day, active night, quiet night.

Profiles are static for the duration of a simulation. Even so-called ultra low frequency waves are still much faster than convective timescales.

TODO: Come up with a characteristic convective timescale or two, and cite it.

4.2.1 Conductivity

The conductivity profiles used in this model are the tabulated values from [11], rescaled by Lysak[4] to account for the increased mean molecular mass at low altitudes.

$$\sigma_P = \sum_s \frac{n_s q_s^2}{m_s}\frac{\nu_s}{\nu_s^2 + \Omega_s^2} \qquad \sigma_H = -\sum_s \frac{n_s q_s^2}{m_s}\frac{\Omega_s}{\nu_s^2 + \Omega_s^2} \qquad \sigma_0 = \sum_s \frac{n_s q_s^2}{m_s \nu_s} \tag{4.9}$$

Each profile is resolved to an altitude of about 1×10^4 km, and include well-resolved E, F_1, and F_2 layers.

TODO: Talk about the ionospheric layers, probably in the introduction.

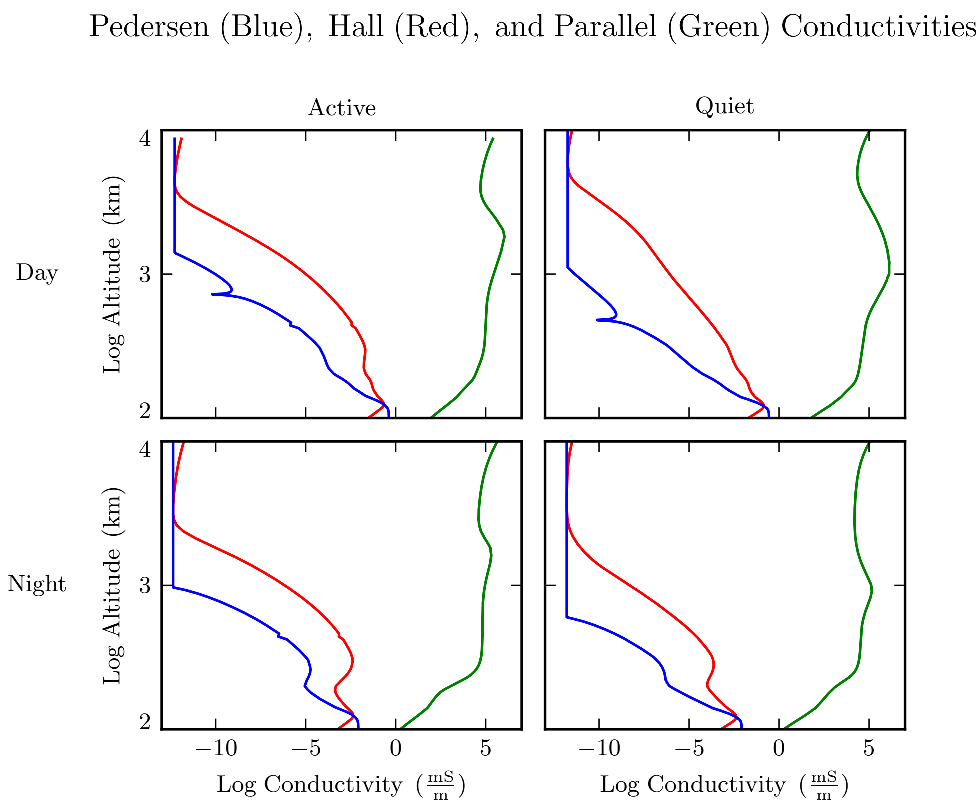

Figure 4.1: Ionospheric conductivity profiles, adapted by Lysak[4] from Appendix B of Kelley's textbook[11].

TODO: What is the height-interated conductivity for each profile?

4.2.2 Alfvén Speed

The Alfvén speed is computed from Kelley's low-density profile, modified to take into account the local density. The density, in turn, is the sum of a plasmaspheric profile and a high-latitude auroral profile.

$$\epsilon_\perp = (\text{low-density tabulated value}) + \frac{n\bar{m}}{B_0^2} \tag{4.10}$$

TODO: What's a clean way of showing the low-density $\epsilon_\perp$ that we read in?

TODO: Above the profile, Bob scales the value that's read in as r^5 or something. Is there a citation for that?

Where $\bar{m}$ is the ambient mean molecular mass and B_0 is the zeroth-order magnetic field strength, $B_0 = 3.11 \times 10^4\,\text{nT}\left(\frac{R_E}{r}\right)^3\sqrt{1 + 3\cos^2\theta}$. Note that $3.11 \times 10^4\,\text{nT}$ is the value of the Earth's magnetic field at the equator on Earth's surface.

TODO: Cite this number?

Note that we do not scale the electric constant to units of ϵ_0.

The Alfvén speed is then computed per equation (3.5), $v_A^2 \equiv \frac{1}{\mu_0 \epsilon_\perp}$.

TODO: Put up a plot of the four Alfvén speed profiles. Show the dipole, or zoom in on the ionosphere?

TODO: Shouldn't the Alfvén speed profiles be brought up early on, since they're necessary for discussions about evanescence at large m in chapter 3?

TODO: Explain in this section how we figure out the time step.

4.3 Maxwell's Equations

The model simulates the evolution of electric and magnetic fields in accordance with Maxwell's equations. Specifically, magnetic fields are advanced using Faraday's Law, and electric fields with Ampère's Law. Kirchhoff's formulation of Ohm's Law ($\underline{J} = \underline{\underline{\sigma}} \cdot \underline{E}$) is used to eliminate the explicit current dependence in Ampère's Law.

$$\frac{\partial}{\partial t}\underline{B} = -\nabla\times\underline{E} \qquad\qquad \underline{\underline{\epsilon}} \cdot \frac{\partial}{\partial t}\underline{E} = \frac{1}{\mu_0}\nabla\times\underline{B} - \underline{\underline{\sigma}} \cdot \underline{E} \tag{4.11}$$

4.3.1 Notation and Optimization

Algebra is carried out on paper, producing expressions where each field value is a linear combination of previous field values. These coefficients are computed before the main loop begins. This offers a significant reduction in floating point operations each iteration.

The $\leftarrow$ operator is used to indicate assignment, rather than equality. Values on the left are new, and those on the right are old. New and old magnetic field values are offset by δt ; electric field values staggered by $\frac{\delta t}{2}$. As an example of this notation, equation (4.12) integrates Faraday's Law over a time step, assuming that the curl of the electric field varies slowly compared to δt :

$$\begin{aligned} \int_0^{\delta t} dt\,\frac{\partial}{\partial t}\underline{B} &= -\int_0^{\delta t} dt\,\nabla\times\underline{E} \\ \underline{B}|_{\delta t} - \underline{B}|_0 &= -\delta t\,\nabla\times\underline{E}|_{\frac{\delta t}{2}} \\ \underline{B} &\leftarrow \underline{B} - \delta t\,\nabla\times\underline{E} \end{aligned} \tag{4.12}$$

It's also beneficial to store the curl of each field, rather than take derivatives on the fly. The following sections make use of the shorthand $\underline{C} \equiv \nabla\times\underline{E}$ and $\underline{F} \equiv \nabla\times\underline{B}$. Or, recalling equation (4.6),

$$C^i = \frac{\varepsilon^{ijk}}{G}\frac{\partial}{\partial u^j}E_k \qquad\qquad F^i = \frac{\varepsilon^{ijk}}{G}\frac{\partial}{\partial u^j}B_k \tag{4.13}$$

Only covariant field components are stored. Only contravariant curl components are stored. This cuts down on memory use, while also eliminating the time spent rotating between bases; those operations are built into the precomputed coefficients.

4.3.2 Magnetic Fields

Taking advantage of the shorthand defined in equation (4.13), Faraday's Law is simply written

$$\frac{\partial}{\partial t}B^i = -C^i \tag{4.14}$$

Or, using the metric tensor to cast the magnetic field in terms of its covariant components, and writing out each coefficient explicitly,

$$\begin{aligned} B_1 &\leftarrow B_1 - g_{11}\,\delta t\, C^1 - g_{13}\,\delta t\, C^3 \\ B_2 &\leftarrow B_2 - g_{22}\,\delta t\, C^2 \\ B_3 &\leftarrow B_3 - g_{31}\,\delta t\, C^1 - g_{33}\,\delta t\, C^3 \end{aligned} \tag{4.15}$$

4.3.3 Electric Fields

Ampère's Law, can be solved with integrating factors. From equation (4.11),

$$\underline{\underline{\epsilon}} \cdot \frac{\partial}{\partial t}\underline{E} = \frac{1}{\mu_0}\nabla\times\underline{B} - \underline{\underline{\sigma}}\cdot\underline{E} \tag{4.16}$$

The permittivity tensor is diagonal, and so can be trivially inverted.

$$\left(\underline{\underline{\Omega}} + \underline{\underline{\mathbb{I}}}\frac{\partial}{\partial t}\right)\cdot\underline{E} = \underline{\underline{v}}^2\cdot\underline{F} \tag{4.17}$$

Where $\underline{\underline{\mathbb{I}}}$ is the identity tensor and in x-y-z coordinates,

$$\underline{\underline{v}}^2 \equiv \frac{1}{\mu_0}\underline{\underline{\epsilon}}^{-1} = \begin{bmatrix} v_A^2 & 0 & 0 \\ 0 & v_A^2 & 0 \\ 0 & 0 & c^2 \end{bmatrix} \quad \text{and} \quad \underline{\underline{\Omega}} \equiv \underline{\underline{\epsilon}}^{-1}\cdot\underline{\underline{\sigma}} = \begin{bmatrix} \frac{\sigma_P}{\epsilon_\perp} & -\frac{\sigma_H}{\epsilon_\perp} & 0 \\ \frac{\sigma_H}{\epsilon_\perp} & \frac{\sigma_P}{\epsilon_\perp} & 0 \\ 0 & 0 & \frac{\sigma_0}{\epsilon_0} \end{bmatrix} \tag{4.18}$$

Using integrating factors, equation (4.17) gives

$$\underline{E} \leftarrow \exp\!\big(-\underline{\underline{\Omega}}\;\delta t\big)\cdot\underline{E} + \delta t\,\underline{\underline{v}}^2\cdot\exp\!\big(-\underline{\underline{\Omega}}\;\tfrac{\delta t}{2}\big)\cdot\underline{F} \tag{4.19}$$

TODO: Do we need to be careful here about the difference between a matrix and a tensor?

The tensor exponential can be evaluated by considering the diagonal and off-diagonal terms separately.

$$\underline{\underline{\Omega}} = \underline{\underline{\Omega}}' + \frac{\sigma_H}{\epsilon_\perp}\begin{bmatrix} 0 & -1 & 0 \\ 1 & 0 & 0 \\ 0 & 0 & 0 \end{bmatrix} \qquad \text{where} \qquad \underline{\underline{\Omega}}' = \begin{bmatrix} \frac{\sigma_P}{\epsilon_\perp} & 0 & 0 \\ 0 & \frac{\sigma_P}{\epsilon_\perp} & 0 \\ 0 & 0 & \frac{\sigma_0}{\epsilon_0} \end{bmatrix} \tag{4.20}$$

Note that tensors are remarkably well-behaved when exponentiated[12], particularly since $\underline{\underline{\Omega}}'$ is diagonal, and thus they commute.

$$\exp\big(\underline{\underline{T}}\big) = \sum_n \frac{1}{n!}\underline{\underline{T}}^n \qquad \text{and} \qquad \exp\big(\underline{\underline{T}} + \underline{\underline{T}}'\big) = \exp\big(\underline{\underline{T}}\big)\exp\big(\underline{\underline{T}}'\big) \tag{4.21}$$

The off-diagonal terms collapse into sines and cosines, indicating a rotation about z.

$$\underline{E} \leftarrow \exp\big(-\underline{\underline{\Omega}}'\,\delta t\big)\cdot\underline{\underline{R}}_z\left(\tfrac{-\sigma_H\delta t}{\epsilon_\perp}\right)\cdot\underline{E} + \delta t\,\underline{\underline{v}}^2\cdot\exp\big(-\underline{\underline{\Omega}}'\,\tfrac{\delta t}{2}\big)\cdot\underline{\underline{R}}_z\left(\tfrac{-\sigma_H\delta t}{2\epsilon_\perp}\right)\cdot\underline{F} \tag{4.22}$$

Where

$$\underline{\underline{R}}_z(\theta) = \begin{bmatrix} \cos\theta & -\sin\theta & 0 \\ \sin\theta & \cos\theta & 0 \\ 0 & 0 & 1 \end{bmatrix} \tag{4.23}$$

The parallel term of term of equation (4.22) is simply

$$E_\parallel \leftarrow E_\parallel \exp\left(\tfrac{-\sigma_0\delta t}{\epsilon_0}\right) + c^2\delta t F_\parallel \exp\left(\tfrac{-\sigma_0\delta t}{2\epsilon_0}\right) \tag{4.24}$$

Or, in covariant terms,

$$E_3 \leftarrow E_3 \exp\left(\tfrac{-\sigma_0\delta t}{\epsilon_0}\right) + c^2\delta t\left(g_{31}F^1 + g_{33}F^3\right)\exp\left(\tfrac{-\sigma_0\delta t}{2\epsilon_0}\right) \tag{4.25}$$

For the ionospheric profiles and time steps employed by this model, $\frac{\sigma_0\delta t}{\epsilon_0}$ is never smaller than 10^3. As a result, $\exp\left(\frac{-\sigma_0\delta t}{\epsilon_0}\right)$ is far too small to be stored in a double precision variable. That is, this simulation takes $E_\parallel$ (and, equally, E_3) to be uniformly zero.

This, obviously, precludes any discussion of parallel electric fields or parallel currents. These topics are revisited in chapter 5.

Not unrelatedly, recalling the definition of the plasma frequency and parallel conductivity from equation (3.5), $\frac{\sigma_0}{\epsilon_0}$ can also be written $\frac{\omega_P^2}{\nu}$.

The plasma frequency is very fast.

The perpendicular components of equation (4.22), mapped from the physical basis to the contravariant basis (per equation (4.7)) to the covariant basis (per equation (4.4)), give

$$\begin{aligned} E_1 + \frac{g^{13}}{g^{11}} E_3 \leftarrow \quad & E_1 \cos\left(\tfrac{-\sigma_H \delta t}{\epsilon_\perp}\right) \exp\left(\tfrac{-\sigma_P \delta t}{\epsilon_\perp}\right) \\ & + E_2 \sin\left(\tfrac{-\sigma_H \delta t}{\epsilon_\perp}\right) \exp\left(\tfrac{-\sigma_P \delta t}{\epsilon_\perp}\right) \sqrt{\frac{g^{22}}{g^{11}}} \\ & + E_3 \cos\left(\tfrac{-\sigma_H \delta t}{\epsilon_\perp}\right) \exp\left(\tfrac{-\sigma_P \delta t}{\epsilon_\perp}\right) \frac{g^{13}}{g^{11}} \\ & + F^1 \cos\left(\tfrac{-\sigma_H \delta t}{2\epsilon_\perp}\right) \exp\left(\tfrac{-\sigma_P \delta t}{2\epsilon_\perp}\right) \frac{v_A^2 \delta t}{g^{11}} \\ & + F^2 \sin\left(\tfrac{-\sigma_H \delta t}{2\epsilon_\perp}\right) \exp\left(\tfrac{-\sigma_P \delta t}{2\epsilon_\perp}\right) \frac{v_A^2 \delta t}{\sqrt{g^{11} g^{22}}} \end{aligned} \tag{4.26}$$

and

$$\begin{aligned} E_2 \leftarrow & -E_1 \sin\left(\tfrac{-\sigma_H \delta t}{\epsilon_\perp}\right) \exp\left(\tfrac{-\sigma_P \delta t}{\epsilon_\perp}\right) \sqrt{\frac{g^{11}}{g^{22}}} \\ & + E_2 \cos\left(\tfrac{-\sigma_H \delta t}{\epsilon_\perp}\right) \exp\left(\tfrac{-\sigma_P \delta t}{\epsilon_\perp}\right) \\ & - E_3 \sin\left(\tfrac{-\sigma_H \delta t}{\epsilon_\perp}\right) \exp\left(\tfrac{-\sigma_P \delta t}{\epsilon_\perp}\right) \frac{g^{13}}{\sqrt{g^{11} g^{22}}} \\ & - F^1 \sin\left(\tfrac{-\sigma_H \delta t}{2\epsilon_\perp}\right) \exp\left(\tfrac{-\sigma_P \delta t}{2\epsilon_\perp}\right) \frac{v_A^2 \delta t}{\sqrt{g^{11} g^{22}}} \\ & + F^2 \cos\left(\tfrac{-\sigma_H \delta t}{2\epsilon_\perp}\right) \exp\left(\tfrac{-\sigma_P \delta t}{2\epsilon_\perp}\right) \frac{v_A^2 \delta t}{g^{22}} \end{aligned} \tag{4.27}$$

The E_3 terms can be ignored at present, but chapter 5 references back to them.

4.4 Driving

If no energy is added, the simulation is pretty boring. Everything just stays zero.

4.4.1 Outer Boundary Compression

Driving from the outer boundary is the traditional way to do it.

TODO: Cite and briefly explain past work done with compressional driving. This is what most of Bob's papers are, right?

As discussed in section 3.4, Alfvén waves become guided when the azimuthal modenumber is large. The energy all stays close to the outer boundary. No field line resonances of significant strength are created within the magnetosphere.

TODO: Show a plot of compressional driving, maybe day and night, as m increases. Mean energy density over time? Something that shows the recession of waves away from the middle of the simulation.

Compressional driving is applied by setting the value of B_3 at the outer boundary.

A compression might reasonably be expected to drive waves with long azimuthal wavelengths. However, there is some indication that waves with short azimuthal wavelength can be driven as well, such as through Kelvin-Helmholtz interactions.

TODO: Find this claim again and cite it.

4.4.2 Ring Current Modulation

Pc4 pulsations with high azimuthal modenumber are known to be driven from within the magnetosphere, such as through drift-resonant interactions with energetic radiation belt and ring current particles.

TODO: Cite.

Substorm injection can cause localized ring current behavior.

TODO: UNH was looking at this at AGU. Check if they have published yet.

During geomagnetically active times, the ring current is a dynamic region. It's easy to imagine localized perturbations.

It's difficult to estimate how large such perturbations might be. The following is a kludgey estimate.

TODO: Plot of Sym-H and its Fourier modes. 1 June 2013. 17 March 2015. 22 June 2015. 17 March 2013. Fit at the "top" of the $\frac{1}{f}$ noise. ("Pink noise"?)

Sym-H is like Dst, but with greater time resolution.

The noise suggests that a Fourier component with a period of about 1 min could have an amplitude around $10^{-3}\,\mathrm{nT}$.

If the driving is delivered at $L = 5$, with a standard deviation of $0.5\,\mathrm{R_E}$ in the radial direction and 5° angularly, that corresponds to a current density of about $4 \times 10^{-4}\,\mathrm{\mu A/m^2}$. This comes from approximating the ring current as a ring of current. Of course, Sym-H is measured at Earth's surface, not at the center of the ring; this gives a geometric factor of about two.

TODO: What electric field magnitude does this correspond to?

Current driving is applied by adding an additional current term. Ampère's Law becomes

$$\underline{\underline{\epsilon}} \cdot \frac{\partial}{\partial t}\underline{E} = \frac{1}{\mu_0}\nabla\times\underline{B} - \underline{\underline{\sigma}} \cdot \underline{E} - \underline{J}_{drive} \tag{4.28}$$

And this driving term is absorbed into the curl by revising equation (4.13) from $\underline{F} \equiv \nabla\times\underline{B}$ to $\underline{F} \equiv \nabla\times\underline{B} - \underline{J}_{drive}$. (As a result, equations (4.26) and (4.27) do not change.)

Notably, Sym-H is a global quantity; it's not ideally suited for making estimates of localized inhomogeneity.

Furthermore, Sym-H has a time resolution of 1 min. It can hardly be said to carry information about oscillations at frequencies of less than two minutes.

Sym-H gives no way to estimate azimuthal modenumber. That's based on Pc4 observations. Dai[2] observed modenumbers approaching 100.

A kludgey estimate is better than no estimate.

4.5 Boundary Conditions

The grid can't go on forever. There have to be special cases at the edges.

4.5.1 Parity and Interpolation

Computation takes place on a staggered grid.

Field values are offset to ensure that most differences are centered. For example, $\frac{\partial}{\partial t}B_2$ depends on $\frac{\partial}{\partial u^1}E_3$ and $\frac{\partial}{\partial u^3}E_1$. If B_2 is defined at even i, E_3 is defined at odd i, so that B_2 is defined on the same grid points as $\frac{E_3[i+1]-E_3[i-1]}{u^1[i+1]-u^1[i-1]}$.

TODO: Make sure the example uses the currect parities.

TODO: Find a citation for the wigglies that occur if field values are defined on all grid points, due to the weak coupling. This problem is apparently well-known.

Values are sometimes needed off-parity. E_1 and E_2 are not defined at the same grid locations, but they are coupled directly by the Hall conductivity. And B_1 and B_3 are coupled by the non-orthogonality of the grid. When off-parity values are needed, they are interpolated from their neighbors.

Differentiation and interpolation are good to second order on the nonuniform grid. Like the coefficients for Maxwell's equations, differentiation and interpolation weights are computed during setup to save time during iteration.

Electric fields go to zero at the innermost and outermost field lines (Dirichlet boundary conditions). Magnetic fields have zero derivative (Neumann boundary conditions). For components not defined at the exact boundary, these rules are applied when differentiating or interpolating; they set the effective value just outside the grid.

These boundary conditions can in principle cause nonphysical reflection at the boundary. In practice, that is not an issue. Wave activity is concentrated well away from the boundaries. In fact, reversing the Dirichlet and Neumann boundary conditions has little effect.

(Of course, an inconsistent boundary condition – like using the same boundary condition for a field and its derivative – causes instability.)

4.5.2 Coupling to the Atmosphere

Conditions at the ionospheric boundaries are set by coupling to the atmosphere. This also allows the computation of ground fields.

It's reasonable to approximate the atmosphere as a perfect insulator, giving $\nabla\times\underline{B} = 0$. Combining with $\nabla \cdot \underline{B} = 0$ per Maxwell's equations, ensures the existence of a scalar magnetic potential Ψ such that $\underline{B} = \nabla\Psi$ and Ψ satisfies Laplace's equation, $\nabla^2\Psi = 0$.

Laplace's equation can be solved analytically; in spherical coordinates, the solutions are spherical harmonics. However, a numerical solution is preferrable to ensure orthonormality on a discrete (and incomplete – there are no grid points at the poles or equator) grid. After separating out the radial and azimuthal dependence in the usual way, the latitudinal component of Laplace's equation (in terms of $s \equiv -\sin^2\theta$) is

$$\left(4s^2 + 4s\right)\frac{d^2}{ds^2}Y_\ell + \left(4 + 6s\right)\frac{d}{ds}Y_\ell - \frac{m^2}{s}Y_\ell = \ell\left(\ell + 1\right)Y_\ell \tag{4.29}$$

Using centered differences to express the derivatives, equation (4.29) is a system of linear equations, one per field line. It can be solved numerically for eigenvalues $\ell\left(\ell+1\right)$ and eigenvectors (harmonics) Y_ℓ. In terms of those harmonics, and noting that the model uses a fixed azimuthal modenumber m , Ψ between R_E and R_I can be expressed

$$\Psi(r, \theta, \phi) = \sum_\ell \left(\alpha_\ell\, r^\ell + \beta_\ell\, r^{-\ell-1}\right) Y_\ell(\theta)\exp(im\phi) \tag{4.30}$$

As a boundary condition for Ψ, Earth's crust is assumed to be a perfect conductor, forcing the magnetic field at the boundary to be perfectly horizontal. That is, $B_r = \frac{\partial}{\partial r}\Psi = 0$. Then, noting that the harmonics Y_ℓ are orthonormal (so each term of the sum must be zero),

$$\beta_\ell = \frac{\ell}{\ell+1} R_E^{2\ell+1} \alpha_\ell \tag{4.31}$$

Note that the explicit ϕ dependence has been dropped. The entire simulation shares a fixed modenumber, so it's sufficient to find Ψ at $\phi = 0$.

At the top of the atmosphere, the radial magnetic field is again used as a boundary condition, this time to compute the weights α_ℓ.

TODO: Something something thin horizontal current sheet at R_I.

Taking the shorthand $\lambda_I \equiv \frac{R_E}{R_I} \sim 0.975$

$$B_r = \sum_\ell \ell\, \alpha_\ell\, R_I^{\ell-1} \left(1 - \lambda_I^{2\ell-1}\right) Y_\ell \tag{4.32}$$

TODO: Settle on good notation for taking the inner product of harmonics. It's a vector in the sense that it's a one-dimensional array of values, but not in the physical sense. Indexing – $B_r\,[i]$ – also seems awkward.

The sum can be collapsed by "integrating" over a harmonic. The inverse harmonics are obtained by inverting the eigenvector matrix. Then $Y_\ell \cdot Y_{\ell'}^{-1} = \delta_{\ell\ell'}$ by construction.

$$\alpha_\ell = \frac{1}{\ell\, R_I^{\ell-1}} \frac{B_r \cdot Y_\ell^{-1}}{1 + \lambda_I^{2\ell+1}} \tag{4.33}$$

Combining equations (4.30), (4.31), and (4.33) allows the expression of Ψ at the top and bottom of the atmosphere as a linear function of the radial magnetic field at the boundary.

$$\begin{aligned} \Psi_E &= \sum_\ell Y_\ell \,\frac{R_I}{\ell} \frac{\frac{2\ell-1}{\ell-1}\lambda^\ell}{1 - \lambda_I^{2\ell+1}} B_r \cdot Y_\ell^{-1} \\ \Psi_I &= \sum_\ell Y_\ell \,\frac{R_I}{\ell} \frac{1 + \frac{\ell}{\ell-1}\lambda_I^{2\ell+1}}{1 - \lambda_I^{2\ell+1}} B_r \cdot Y_\ell^{-1} \end{aligned} \tag{4.34}$$

Magnetic fields are evaluated from Ψ per

$$B_1 = \frac{\partial}{\partial u^1}\Psi \qquad\qquad B_2 = \frac{\partial}{\partial u^2}\Psi \tag{4.35}$$

Note that B_1 and B_2 are horizontal; per equation (4.8), they are proportional to B_θ and B_ϕ respectively.

At the ground, field values are purely output.

Horizontal magnetic field values at the top of the ionosphere, on the other hand, are used as boundary conditions. Assuming there is no vertical component to the ionospheric current sheet, the electric field values at the ionospheric edge of the grid are dictated by the jump in horizontal magnetic field between the bottom of the grid and the top of the atmosphere.

$$\mu_0 \, \underline{\underline{\Sigma}} \cdot \underline{E} = \lim_{\delta r \to 0} \hat{r} \times \underline{B} \Big|_{R_I - \delta r}^{R_I + \delta r} \tag{4.36}$$

TODO: Bob's citations for the ionospheric jump conditions: Fujita and Tamao 1988, Yosikawa and Itonaga 1996, 2000, Lysak and Song 2001, Sciffer and Waters 2002. It basically comes from integrating Ampère's Law, so half a dozen citations seems like overkill.

Chapter 5

Electron Inertial Effects

TODO: Bob mentions something about electron inertia or pressure being in his 2011 paper.

The model described in chapter 4 has the notable omission of parallel electric fields and parallel currents. That situation can be remedied by the addition of the electron inertial term in Ohm's Law.

Old parallel electric field formulation. Recall $\underline{F} \equiv \nabla \times \underline{B}$.

$$\epsilon_0 \frac{\partial}{\partial t} E_\parallel = \frac{1}{\mu_0} F_\parallel - \sigma_0 E_\parallel \tag{5.1}$$

New parallel electric field formulation. The parallel current must now be tracked explicitly.

$$\epsilon_0 \frac{\partial}{\partial t} E_\parallel = \frac{1}{\mu_0} F_\parallel - J_\parallel \qquad\qquad \frac{\partial}{\partial t} J_\parallel = \frac{n e^2}{m} E_\parallel - \nu J_\parallel \tag{5.2}$$

In the new formulation, $J_\parallel$ (equally, J_3) is solved with integrating factors and $E_\parallel$ (E_3)

can be advanced directly.

$$\begin{aligned} E_3 &\leftarrow E_3 + c^2 \delta t \, \left(g_{31} F^1 + g_{33} F^3 \right) - \frac{\delta t}{\epsilon_0} J_3 \\ J_3 &\leftarrow J_3 \exp(-\nu \delta t) + \frac{ne^2}{m} \delta t \, E_3 \exp\left(-\nu \tfrac{\delta t}{2}\right) \end{aligned} \tag{5.3}$$

Recall that the electric and magnetic fields are staggered by half a time step. The current is defined with the magnetic fields, offset from the electric fields.

5.1 The Boris Approximation

Note that

$$\frac{\partial}{\partial t} E_\parallel \sim -\frac{1}{\epsilon_0} J_\parallel \qquad \text{and} \qquad \frac{\partial}{\partial t} J_\parallel \sim \frac{ne^2}{m_e} E_\parallel \qquad \text{so} \qquad \frac{\partial^2}{\partial t^2} E_\parallel \sim -\omega_P^2 E_\parallel \tag{5.4}$$

That is, the addition of the electron inertial term in Ohm's Law allows plasma oscillations.

As noted in section 4.3.3, the plasma frequency is very large. Much larger than $\frac{1}{\delta t}$. But $\omega_P \delta t < 1$ is necessary for stability. In order to accommodate that condition, the time step in some runs would need to be dropped by three orders of magnitude; a simulation slated for one hour would suddenly take six weeks to complete.

The time step dictated by the Alfvén speed and grid spacing is typically on the order of 10 µs, while the plasma frequency can be as small as 10 ns.

But there is another way into Mordor. There's a path, and some stairs and then a tunnel.

The plasma frequency (and the speed of light) can be decreased by taking an artificially large value for ϵ_0 .

Such approximations have been staples of numerical MHD models since Boris' work in 1970[13].

Lysak and Song[3] demonstrate the validity of such an approximation. To paraphrase their work, take equation (5.2) and suppose that $E_\parallel$ and $J_\parallel$ are oscillating at a frequency ω. Then,

$$-i\omega\epsilon_0 E_\parallel = \frac{1}{\mu_0}F_\parallel - J_\parallel \qquad\qquad -i\omega J_\parallel = \frac{ne^2}{m_e}E_\parallel - \nu J_\parallel \tag{5.5}$$

So

$$\left(1 - \frac{\omega^2 - i\nu\omega}{\omega_P^2}\right) E_\parallel = \frac{c^2}{\omega_P^2}\left(\nu - i\omega\right) F_\parallel \tag{5.6}$$

Here $\frac{c}{\omega_P}$ is the electron inertial length. While the speed of light and the plasma frequency each depend on ϵ_0 , their ratio does not. So long as $\left(1 - \frac{\omega^2 - i\nu\omega}{\omega_P^2}\right) \sim 1$, a change in ϵ_0 should not affect model behavior.

For the purposes of simulating ultra low frequency waves, equation (5.6) allows perhaps-implausibly large Boris factors; even increasing ϵ_0 by a factor of 10^6 gives $\left|\frac{\omega^2 + i\omega\nu}{\omega_P^2}\right| \lesssim 0.01$. At that point, in some places, the speed of light is significantly slower than the Alfvén speed.

TODO: Ronnmark[14] calls this "anisotropic vacuum."

TODO: Show a plot of these frequency ratios in the ionosphere?

TODO: Generalized Ohm's Law, in case we decide we need it. Could talk through why all of the other terms are OK to neglect.

$$\underline{E} + \underline{U}\times\underline{B} = \eta\underline{J} + \frac{m_e}{ne^2}\left[\frac{\partial}{\partial t}\underline{J} + \nabla\cdot\left(\underline{J}\,\underline{U} + \underline{U}\,\underline{J} + \frac{1}{ne}\underline{J}\,\underline{J}\right)\right] + \frac{1}{ne}\underline{J}\times\underline{B} - \frac{1}{ne}\nabla\cdot\underline{\underline{P_e}} \tag{5.7}$$

...

...

...

5.2 Field-Aligned Currents

5.3 Inertial Length Scales

Chapter 6

Large Modenumber Effects

This is why we do 2.5D... you can't resolve these effects in a 3D model. It's too expensive.

TODO: Do we see a difference between $\underline{k}$ (momentum) and the group velocity? Poynting flux will always be pretty much along the field line, since B_3 is small and E_3 is zero, but the wave vector need not be. This is a question of coupling/converting to compressional waves, I guess.

TODO: Look at McKenzie and Westphal. Waves incident on the bow shock, etc, at weird angles.

TODO: Look at the E to B ratio. Compare to the Alfvén speed and to the height-integrated Pedersen conductivity.

6.1 Finite Poloidal Lifetimes

CITE RADOSKI 1974

CITE MANN 1995

CITE DING 1995

TODO: Look at Mann's poloidal lifetime, $\frac{\partial}{\partial \omega_A'} \lambda$ where $\lambda \sim \frac{m}{2\pi r}$.

6.2 Development of Fine Structure

6.3 Damping of Ground Signatures

6.4 Electromagnetic Energy Gap

Chapter 7

Evolution of Giant Pulsations

Chapter 8

Comparison to Van Allen Probe Observations

TODO: Note that RBSP's ability to measure poloidal/toroidal waves depends on geometry. It always has to guess for one electric field component.

Chapter 9

Conclusion and Discussion

9.1 Future Work

Non-sinusoidal driving, obviously.

Arbitrary deformation of grid. Get $\hat{e}_i = \frac{\partial}{\partial u^i}\underline{x}$, then $g_{ij} = \hat{e}_i \cdot \hat{e}_j$, then invert.

3D using MPI.

References

[1] Lei Dai, Kazue Takahashi, John R. Wygant, Liu Chen, John Bonnell, Cynthia A. Cattell, Scott Thaller, Craig Kletzing, Charles W. Smith, Robert J. MacDowall, Daniel N. Baker, J. Bernard Blake, Joseph Fennell, Seth Claudepierre, Herbert O. Funsten, Geoffrey D. Reeves, and Harlan E. Spence. Excitation of poloidal standing alfvén waves through drift resonance wave-particle interaction. *Geophys. Res. Lett.*, 40:41274132, 2013.

[2] Lei Dai, Kazue Takahashi, Robert Lysak, Chi Wang, John R. Wygant, Craig Kletzing, John Bonnell, Cynthia A. Cattell, Charles W. Smith, Robert J. MacDowall, Scott Thaller, Aaron Breneman, Xiangwei Tang, Xin Tao, and Lunjin Chen. Storm time occurrence and spatial distribution of pc4 poloidal ulf waves in the inner magnetosphere: A van allen probes statistical study. *J. Geophys. Res. Space Physics*, 120:47484762, 2015.

[3] Robert L. Lysak and Yan Song. A three-dimensional model of the propagation of alfvén waves through the auroral ionosphere: first results. *Adv. Space Res.*, 28:813–822, 2001.

[4] Robert L. Lysak, Colin L. Waters, and Murray D. Sciffer. Modeling of the ionospheric alfvén resonator in dipolar geometry. *J. Geophys. Res. Space Physics*, 118, 2013.

[5] M. J. Engebretson, L. J. Zanetti, T. A. Potemra, W. Baumjohann, H. L uhr, and M. H. Acuna. Simultaneous observation of pc 34 pulsations in the solar wind and

in the earth's magnetosphere. *J. Geophys. Res. Space Physics*, 92:10053–10062, 1987.

[6] Henry R. Radoski. A note on oscillating field lines. *J. Geophys. Res.*, 72(1), 1967.

[7] Jeffrey A. Proehl, William Lotko, Igor Kouznetsov, and Shireen D. Geimer. Ultralow-frequency magnetohydrodynamics in boundary-constrained geomagnetic flux coordinates. *J. Geophys. Res.*, 107(A9):1225, 2002.

[8] Robert L. Lysak. Magnetosphere-ionosphere coupling by alfvén waves at midlatitudes. *J. Geophys. Res.*, 109, 2004.

[9] W. D. D'haeseleer, W. N. G. Hitchon J. D. Callen, and J. L. Shohet. *Flux Coordinates and Magnetic Field Structure*. Springer-Verlag, New York, 1991.

[10] A. Einstein. Die grundlage der allgemeinen relativit atstheorie. *Ann. Phys.*, 354:769–822, 1916.

[11] Michael C. Kelley. *The Earth's Ionosphere*. Academic Press, San Diego, second edition, 1989.

[12] Brian C. Hall. *Lie Groups, Lie Algebras, and Representations*. Graduate Texts in Mathematics. Springer, New York, second edition, 2015.

[13] Jay P. Boris. A physically motivated solution of the alfvén problem. *NRL Memorandum Report*, 2167, 1970.

[14] Kjell R onnmark and Maria Hamrin. Auroral electron acceleration by alfvén waves and electrostatic fields. *J. Geophys. Res.*, 105:25333–25344, 2000.

Appendix A

Differential Geometry

Care has been taken in this thesis to minimize the use of jargon and acronyms, but this cannot always be achieved. This appendix defines jargon terms in a glossary, and contains a table of acronyms and their meaning.

A.1 Glossary

- **Cosmic-Ray Muon** (**CR** μ) – A muon coming from the abundant energetic particles originating outside of the Earth's atmosphere.

A.2 Acronyms

Table A.1: Acronyms

Acronym	Meaning
CRμ	Cosmic-Ray Muon

Appendix B

Integrating Factors

Start with differential equation of the form:

$$\frac{\partial}{\partial t}X(t) + \alpha X(t) = \beta \tag{B.1}$$

Multiply by the integrating factor, then group terms:

$$\exp(\alpha\ t)\frac{\partial}{\partial t}X(t) + \alpha \exp(\alpha\ t)X(t) = \beta \exp(\alpha\ t) \tag{B.2}$$
$$\frac{\partial}{\partial t}\big[\exp(\alpha t)X(t)\big] = \beta \exp(\alpha t) \tag{B.3}$$

Integrate from 0 to δt, assuming that β is constant in time or varies slowly.

$$\int_0^{\delta t} dt \frac{\partial}{\partial t}\big[\exp(\alpha t)X(t)\big] = \int_0^{\delta t} dt\beta \exp(\alpha t) \tag{B.4}$$
$$\exp(\alpha\delta t)X(\delta t) - X(0) = \delta t\beta(\frac{\delta t}{2})\exp(\alpha\frac{\delta t}{2}) \tag{B.5}$$

Then rearrange to solve for the new value of X:

$$X(\delta t) = X(0)\exp(-\alpha\delta t) + \delta t\beta(\frac{\delta t}{2})\exp(-\alpha\frac{\delta t}{2}) \tag{B.6}$$

Done.